Real-Time Microscopy of Reorientation Driven Nucleation and Growth in Pentacene Thin Films on Silicon Dioxide

*Abdullah Al-Mahboob, Yasunori Fujikawa, Toshio Sakurai, and Jerzy T. Sadowski**

The role of molecular reorientation processes in the self-assembly of anisotropic molecules, such as pentacene (Pn) is studied utilizing a unique capability of low-energy electron microscopy (LEEM) for the real-time investigation of the film growth. In Pn film on SiO_2, a layer-by-layer growth is observed, albeit different from the expected Volmer–Weber growth mode typical for the systems with lower adhesion (weak interfacial interaction). The observed growth mechanism is also different than conventional concept of layer-by-layer, or Frank van der Merwe growth. In the Pn/SiO_2 system the nucleation density decreases in each consecutive layer, at least up to four monolayers. This growth mechanism is hereafter named inverse Stranski-Krastanov growth. Furthermore, in this growth system the second layer islands nucleate preferentially at the domain boundaries formed by the interconnections of the bottom (first layer) domains. The top layer overgrows bottom layer with its own, initial in-plane crystal orientation, regardless of the in-plane orientations in underlying Pn domains. The dark-field LEEM imaging allows us to distinguish between Pn domains having different azimuthal direction of molecular tilt. LEEM intensity versus start voltage (LEEM *I–V*) curves taken in the vicinity of mirror potential from the first and second layer Pn islands show that the surface potential of the second layer is higher by about 0.05 eV than that of the first layer, while the surface potentials for the epitaxial and non-epitaxial parts of the second layer island are identical.

1. Introduction

Recent progress in the field of organic electronic devices receives significant attention due to their potential for low cost, facile manufacturing, underscoring its importance for the microelectronic industry. Among currently investigated organic materials, pentacene (Pn, $C_{22}H_{14}$) appears to be particularly interesting, since in terms of field-effect mobility, Pn-based devices are comparable to,[1] or even better[2] than those made of amorphous silicon. The record RT hole mobility in organic devices made of single crystal Pn is as high as 35 $cm^2\ V^{-1}\ s^{-1}$.[3] However, the carrier mobility in Pn thin film field-effect transistors (FETs) is at best at the order of ≈1 $cm^2\ V^{-1}\ s^{-1}$,[4] which can be explained by the lack of a control over the crystallinity of organic thin films, defects at interface and high density of domain boundaries.

Pentacene molecules form layered crystal structures in both, bulk[5] and thin film phases,[6] where the molecules are arranged in a tilted, standing-up orientation, with a surface generally defined as (001) or *ab*-plane, being the most stable crystal face.[7] The schematic of the Pn unit cell with the outlay of the in-plane lattice vectors is shown in **Figure 1**. When deposited on noble metals,[8–11] Pn adsorbs in a lying-down configuration, whereas on insulating,[12] or semiconducting/semimetallic inorganic surfaces,[13–16] Pn films are terminated with a standing-up molecular orientation (the *ab*-plane being parallel to the substrate surface). In bottom-contact FET structures containing both, metallic and insulating surfaces, such substrate-dependent molecular ordering often leads to growth defects at the boundary between metal contacts and the dielectric. This problem can be solved by tuning the interfacial interaction between electrode and Pn molecules through the modification of the electrode surface.[17]

Specifically, the quality of first few, nearest to the substrate Pn layers, is crucial for device performance.[18] It has been shown that an anisotropy in molecular structure greatly influences growth kinetics of organic thin films,[13,19–23] and thus affects their crystallinity. In our previous investigation we have found that in case of vacuum deposited Pn the growth anisotropy of self-organized Pn film is related to kinetic processes, rather than to thermodynamics, irrespective of the presence, or lack of epitaxial commensuration with the substrate.[13] We have shown that Pn film growth is governed by slow kinetic incorporation process, caused by an energy barrier for molecule reorientation (hereafter the reorientation-limited growth), which can result in a formation of giant single crystalline Pn islands.[19] The concept of such reorientation process in the self-assembly of Pn film is illustrated in **Figure 2**. In the case of inorganic film growth with symmetric atom as a growth unit,

Dr. A. Al-Mahboob, Dr. J. T. Sadowski
Center for Functional Nanomaterials
Brookhaven National Laboratory
Upton, NY 11973, USA
E-mail: sadowski@bnl.gov
Dr. Y. Fujikawa
Institute for Materials Research
Tohoku University
2-1-1 Katahira, Aoba-ku, Sendai 980-8577, Japan
Prof. T. Sakurai
WPI-Advanced Institute for Materials Research
Tohoku University
2-1-1 Katahira, Aoba-ku, Sendai 980-8577, Japan

DOI: 10.1002/adfm.201203427

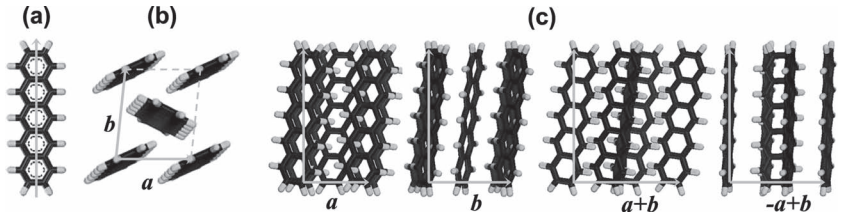

Figure 1. a) Sketch of the Pn molecule; LMA stands for the direction of long molecular axis; b) top view and c) several different side views of the Pn unit cell with the outlay of in-plane lattice vectors.

the nucleation, growth anisotropy and growth modes can be determined respectively by diffusivity, step energies and orientation independent interfacial energies. Situation can be more complicated in case of organic film growth. Because of its planar structure, an isolated, diffusing Pn molecule is expected to be lying-down on a flat substrate surface, as the interaction in this configuration can be maximized (Figure 2b). On the other hand, after self-assembly into the thin film the Pn molecules are standing-up with the (001) plane as the surface.[24] Larger interface interaction results in longer diffusion time and thus larger equilibrium density of diffusing molecules.

In this work we investigate in detail role of molecular anisotropy and strength of interfacial interactions in controlling of the nucleation and growth of vacuum deposited Pn thin films. We show that the mechanisms of nucleation and growth in organic film can deviate from the classical models developed for inorganic film growth.[25–27] We also report on details of molecular ordering and twinning in Pn films on SiO_2.

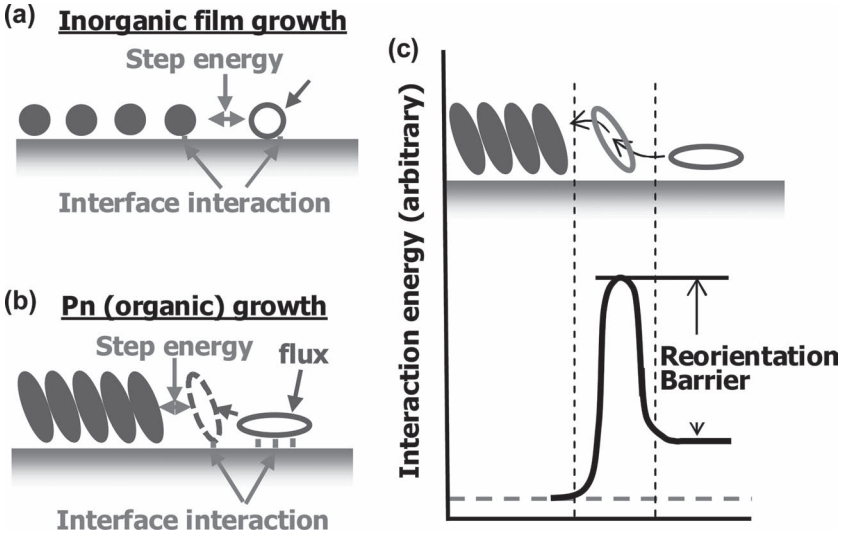

Figure 2. Schematics depicting the comparison between growth and nucleation processes in inorganic and organic anisotropic molecular system such as Pn film: a) Interfacial interaction for a diffusing atom is similar as that for an atom at the step edge thus the nucleation and island evolution can be determined from diffusivity, attachment-detachment energy barriers and step energies; b) Interfacial interaction for diffusing lying-down molecules (i.e., Pn) is different than that at the step edge; c) The strength of interfacial interaction at the diffusion state determines the energy barrier for reorientation, such that the stronger interaction increases the relative stability of diffusing molecules.

2. Results and Discussion

2.1. Mechanism of Nucleation and Growth Modes of Pentacene

In course of our experiments we have extensively examined the growth of pentacene on SiO_2 at various growth conditions, varying deposition rates and substrate temperatures. For the substrate temperatures from room temperature (RT) to about 80 °C, Pn was observed to grow in a layer-by-layer mode, at least up to completion of the third layer. When the substrate was kept at RT, completion of the first standing-up layer and completion of the second layer after its nucleation begun required almost identical amount of nominal deposition, indicating lack of formation of a wetting layer. With increase in the substrate temperature, time required for the completion of the first ML (at the same deposition rate) gradually became longer due to thermal desorption of Pn from the weakly interacting SiO_2. The completion of the first ML also took longer than the completion of the second ML, indicating that the interaction between Pn and SiO_2 is weaker than that between Pn molecule and Pn terraces (layers). Series of low-energy electron microscopy (LEEM) images obtained during such a layer-by-layer growth of Pn on SiO_2 at a substrate temperature of 65 °C is shown in **Figure 3**. From these LEEM data it is also apparent that the nucleation density for the second layer islands is lower than that for the first layer, and even more so, the density of the third layer Pn islands is lower than that for the second layer.

According to classical thin film growth theory, the initial layer-by layer or Frank-van der Merwe (FM) growth[25] should be a characteristics of a stronger interfacial adhesion between first layer and substrate, rather than the interlayer cohesion between first and second layer. In general, after formation of initial stabilizing layer (i.e., weakening the interaction with the substrate), the local growth instabilities result in Stranski–Krastanov (SK) growth. Because of the existence of the Ehrlich–Schwoebel (ES) barrier (70 meV in case of Pn[28,29]), which increases the concentration of the diffusing molecules on the terraces, the growth should turn soon into SK growth,[26] i.e., gradual increase in nucleation density of the islands in subsequent layers should be observed. In fact, we have observed the opposite—a gradual decrease of nucleation density when the number of layers increases. We will call this phenomenon an inverse Stranski–Krastanov (inverse-SK) growth.

As discussed above, the interfacial adhesion between SiO_2 and Pn is much weaker than the interlayer cohesion between first and second pentacene layers, which was observed also in the previous work.[30] One

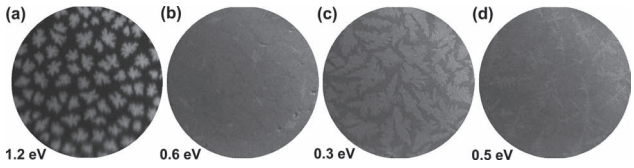

Figure 3. Time series LEEM images recorded during Pn deposition on SiO_2 at substrate temperature of 65 °C: a) first layer Pn islands; b) onset of the nucleation of second layer islands; c) second layer islands on first layer; and d) third layer islands on the second layer, respectively. The field-of-view for all images is 30 µm.

could speculate that this energetic balance should result in initial 3D or Volmer–Weber (VW)[27] growth within the regime of classical film growth. In fact we seldom observe a growth of Pn bilayer (primarily on surfaces not treated with plasma), which is, in any case, subsequently followed by the inverse-SK growth. In order to understand this nucleation and growth process we have proposed a reorientation-limited film growth model.[19,31] According to this model, the energy barrier for the film growth includes both, an energy barrier for molecule reorientation from lying-down, diffusive state to standing-up orientation (a transition state, TS), and a barrier for molecule attachment at the island edges. The attachment energy barriers for molecule to incorporate from TS into an island are independent of substrate for a given Pn polymorph, while the energy barrier for reorientation is substrate-dependent, i.e., stronger adhesion makes energy barriers for the reorientation larger. This reorientation barrier strongly influences the nucleation and growth processes in Pn films. It should be noted here that if the interfacial interaction is too strong, incorporation barrier becomes too high to overcome, which prevents Pn molecules from standing up at the first layer, as it has been observed in Pn grown on C_{60}(111) surface,[32] or Pn deposited on noble metals.[8,9] On moderately interacting surfaces, the presence of the reorientation barrier makes the probability for a molecule to be standing-up lower than the one on a weaker interacting surface, which in turn results in the attachment of molecules at the island edges being slower for the identical molecular concentration on the surface. In order to form a critical nucleus of size i, a standing-up molecule needs at least additional (i-1) standing-up molecules at the closest neighborhood. According to the scaling analysis by Stadlober et al.,[33] for the Pn it is $3 \leq i \leq 4$. As the interaction between Pn molecule and first Pn layer is stronger that that between Pn and SiO_2 substrate, the nucleation probability for the second layer becomes lower and the inverse-SK growth is observed in the second layer.

In separate set of LEEM experiments, we have determined that the second layer nucleates preferentially at the domain boundaries (DBs) formed by connections of the first layer islands. This is due to fact that high defect density at DBs results in a longer residence time for Pn molecule in comparison with that at the center of domain. This longer residence time of Pn molecules at DBs makes the local molecular density gradually higher as additional molecules are being supplied by deposition and diffusion, so there is a greater chance to reach critical molecular concentration to form an island there.

As noted above, the nucleation density of subsequent layers is further lowered. This is caused by: (1) a decrease in density of grain boundaries, which allows the molecules diffuse freely, and (2) an increase in the interlayer cohesion (lowest for the thin-film phase, highest fro the bulk-terminated surface). After certain number of layers is grown and the interlayer cohesion does not change anymore, we do not expect further decrease in nucleation density due to the reorientation barrier. Instead, the ES barrier might be effective in increasing the density of diffusing molecules on the terraces, and thus the growth mechanism changes from inverse-SK to SK one. In fact the presence of the SK-growth in the thicker Pn films on SiO_2 has been documented in literature.[34] The fact that the inter-layer cohesion increases with the film thickness, was confirmed by our calculations of the inter-layer energies between the neighboring layers of Pn. The calculations were performed for bilayer Pn with a vacuum slab. We considered various in-plane lattice parameters to account for thin film phases,[6] a ML Pn on SiO_2,[35] a ML Pn on H-Si(111),[14] and the bulk phase (Holmes).[36] According to previous studies, the in-plane lattice parameters vary little between different thin film phases and the magnitude of in-plane lattice vectors, as well as molecular tilt at (001) plane increase from a thin film phase Pn to a bulk-terminated Pn.[6,37] From earlier experiments reported by Cheng et al. it is known that both, molecular tilt and the surface energies of Pn on SiO_2 increase with the film thickness.[37] Our density functional theory (DFT) calculations further indicated that an increase in inter-layer cohesion is related to the increase in molecular tilt. Therefore the gradual increase in cohesion and observed preference in nucleation at DBs at lower thickness suggest that the combination of both, change in the inter-layer energy at subsequent layers and limited diffusion at grain boundaries, are responsible for the inverse-SK growth. At elevated temperatures, when the activation to standing-up TS on SiO_2 substrate is easier, interfacial adhesion and inter-layer cohesion will dominate over reorientation processes. Thus the film growth is expected to be governed in accordance with well established classical models, and we should observe the VW growth. In fact we have seen such 3D growth in our experiments, when Pn was deposited at substrate kept at around 120 °C. Similar 3D growth of Pn films grown on alkylated substrates SiO_2 at elevated temperature is reported elsewhere.[38]

To further confirm our claim that nucleation and film growth mechanism of Pn film grown on substrate kept at close to RT is associated with the reorientation processes rather than classical concept of interfacial adhesion/inter-layer cohesion, we have grown Pn on semimetallic and semiconducting substrates, in which cases the interfacial adhesion is somewhat stronger than that on SiO_2. According to previous reports,[19] nucleation density of standing-up Pn at RT on such substrates is very low because of large reorientation energy barrier, and the first layer island density on well ordered substrates is as much as six orders of magnitude lower than that observed on SiO_2 substrates. Typical example of a growth of Pn on semiconducting $\alpha\sqrt{3}$-Bi-Si(111) is shown in the LEEM images in **Figure 4**. In this case we expect similar Pn inter-layer cohesion as in the Pn/SiO_2 system, but still being weaker than the interfacial adhesion. Interestingly, in this case the observed growth mode somewhat resembles the SK-type–the nucleation density in the top layer is several orders of magnitude higher than in the first layer. The second layer island density is comparable to

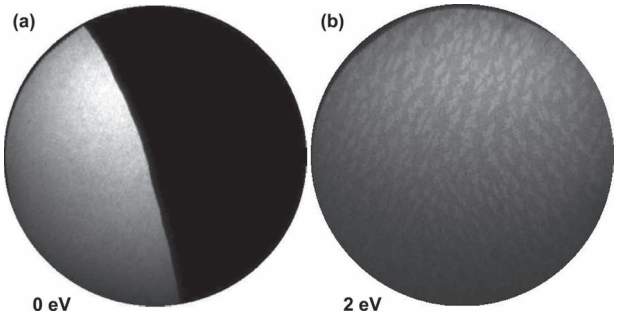

Figure 4. LEEM images of sub-ML Pn grown on $\alpha\sqrt{3}$-Bi-Si(111) at RT: a) step-flow growth of the first layer Pn island (bright); and b) second layer islands (brighter) on top of the first layer Pn. The field-of-view for both images is 30 μm.

that for second and third layer Pn on SiO_2. This observation again implies the validity of proposed mechanism, in which the nucleation and Pn film growth on SiO_2 are predominantly determined by the molecule reorientation-limited processes.

2.2. Molecular Ordering and Twinning in Pn Films

In the previous section we have shown that the second layer Pn on SiO_2 or inert dielectric surfaces has lower nucleation density than that of the first layer, which is driven by molecule reorientation-limited processes. Another important observation is that the second layer islands overgrow first layer keeping their own initial in-plane crystal lattice orientation, regardless of in-plane lattice orientation of the bottom layer, even as they spread over several randomly oriented grains. In such case, the misalignment between overlayer and a bottom layer lattices should increase the inter-layer energy. On the other hand, if Pn island has to follow the bottom layer lattice registry, the in-plane lattice orientation is required to change when the growth front of second layer island moves forward from the terrace of one first layer island to another one. Such process will increase the energy of the film by the cost of the formation of lattice mismatch within the second layer. According to the DFT calculations (local density functional (LDA) approach), the interlayer binding energy (480 meV per unit cell) within the free-standing double layers (BL) is almost one order of magnitude smaller than intermolecular binding energy within a layer (3.2 eV per unit cell). This results in smaller energy cost for inter-layer mismatch at growth front in comparison to that for creation of additional domain boundaries in the top layer. Therefore the crystal orientation of second layer remains stable during island evolution regardless of the orientation in the bottom layer.

The interlayer electronic coupling varies because of locally different relative azimuthal orientations of first and second layers. This can influence the quality of crystalline ordering within the islands in the top layers and thus the electronic properties of pentacene thin film. This difference in crystallinity is evident in the bright-field LEEM images shown in **Figure 5**. In the bright-field LEEM image taken under normal imaging conditions there is no discernible contrast within a second layer island (Figure 5a). However, when the electron beam is slightly tilted from the surface normal, clear relative contrast within various portions of second layer islands appears in the LEEM image shown in Figure 5b, illustrating rather complex epitaxial relations between the second and first layer.

To analyze such surface potential shifts in greater detail, we analyzed the LEEM intensity versus start voltage (LEEM *I–V*) curves from the first and second layer Pn islands, where the start voltage (which defines effective kinetic energies of electron at the sample surface) was varied around the one corresponding to mirror mode imaging conditions.[39] In this mode, when the imaging electrons have energies lower than the

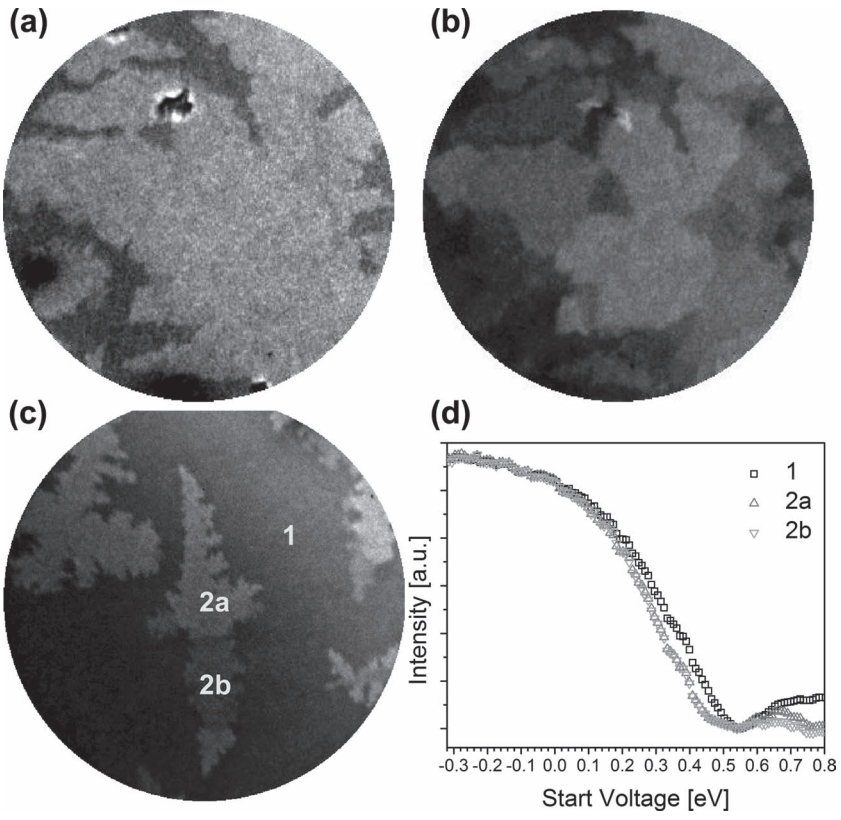

Figure 5. a) Bright-field LEEM image showing second layer Pn (bright) on first layer (gray) grown at 75 °C on SiO_2–no apparent contrast within the island is visible in this imaging mode; b) Bright-field LEEM image of the island shown in (a) with the electron beam tilted in an arbitrary direction–this time a contrast is visible within an island, which is associated with locally different relative in-plane orientations between second layer island and first Pn layer; c) LEEM image showing second layer islands on Pn/SiO2 grown at 55 °C taken at similar imaging conditions as (b); d) LEEM *I–V* curves taken from the first layer (labeled "1") and two different areas of the second layer island (labeled "2a" and "2b", respectively); The imaging electron energy is 0.4 eV, 2.5 eV and 1.0 eV in (a), (b) and (c), respectively, while field-of-view is 10 μm in all LEEM images.

mirror potential value, they are reflected back before reaching the sample surface, resulting in the high intensity in the corresponding LEEM image. At a start voltage corresponding to a mirror potential, the electrons just reach the sample surface, and the reflected or backscattered intensity is lowest. When the start voltage exceeds the mirror potential, the energy-dependent reflectivity and diffractive scattering cause the local intensities in the LEEM image to vary, depending on the local elemental and crystallographic structure of the surface. Changes in the apparent mirror potential (changes in start voltage corresponding to mirror imaging conditions) in the LEEM images directly correspond to the shift in the effective surface potential, i.e., shift of the start voltage towards lower values indicates higher surface potential of the sample. In a number of the LEEM studies, such potential shift towards lower value is regarded as corresponding to lowering of the work function of the surface.[40]

A tilted-beam LEEM image taken from the Pn film on SiO_2 composed of few second layer islands (brighter) on top of full first layer (darker) is shown in Figure 5c. Additional relative contrast is visible between epitaxial (brighter) and non-epitaxial (darker) part of the second layer island (areas 2a and 2b in Figure 5c, respectively). The LEEM *I–V* curves taken from the first layer and different parts of the second layer island are shown in Figure 5d. One can clearly see that the surface potential of the second layer is higher by about 0.05 eV in relation to that of the first layer, while there is no difference in the surface potentials for the epitaxial and non-epitaxial parts of the second layer island.

This is in partial agreement with an earlier work by Kalihari et al.,[41] who reported on the local electrostatic potential differences for variously oriented second layers of Pn in Kelvin probe force microscopy (KFM) measurements. They concluded that the second layer has a positive potential with respect to the underlying layer, and the second layer domains that are epitaxially aligned with the first layer have significantly more positive surface potential than the non-epitaxial domains.

Interestingly, a photoemission electron microscopy (PEEM) image in **Figure 6**a, taken with a Hg arc lamp as an UV excitation source, shows darker contrast for the second layer islands, than this of the first layer. This may imply that the work function of the second Pn layer is higher that that of the first layer, however we cannot exclude the attenuation of the emission from the substrate by elastic and inelastic scattering of the emitted substrate electrons migrating through the organic layer. The corresponding LEEM image, taken from the same surface areas, is shown in Figure 6b.

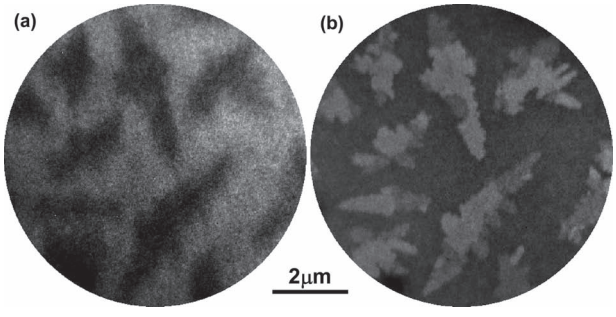

Figure 6. a) Threshold PEEM image and b) a bright-field LEEM image (taken at 1.7 eV) of the same area showing second layer islands; the second layer islands appear darker than the first layer in the PEEM image.

The relative orientation between first layer and second layers affects the crystallinity and out-plane electronic coupling, which in turn influences the out-plane electronic transport properties, such as bias induced dipole, or charge injection, and out-plane carrier hopping. Therefore, the epitaxial relation between Pn layers affects device properties as well as contributes to the contrast between epitaxially matched and mismatched layers in the Kelvin-probe measurements.

We have reported previously that the molecular tilt in the Pn layer with respect to surface normal introduces asymmetry in micro-beam low-energy electron diffraction (μ-LEED) patterns at very low kinetic energies of incident electrons.[16] This property can be used for spatially-resolved LEEM mapping of molecular tilt in Pn films. In the case of Pn on SiO_2, the molecular tilt is very small. The calculations indicate that it is 1.1° for free-standing, thin-film like Pn ML on SiO_2, and 9° for the free-standing, bulk-like Pn ML. Despite that, by slightly varying the electron beam tilt in regard to the surface plane, the imaging conditions can be tuned to obtain imaging contrast between different second layer islands, that have random relative in-plane lattice orientations. Similar contrast variation is also found between epitaxial and non-epitaxial portion of a second layer island that overgrows several different first layer islands. Analogous to a grain boundary, the interlayer mismatch can introduce tilt domain boundaries and can affect an intra-layer carrier transport, in addition to influencing the interlayer electronic coupling.

It is interesting to see what is the epitaxial relation between first and second layer in Pn film on SiO_2 if the nucleation of the second layer island occurs at the center of the first layer domain, rather than at the DB. In this experiment, initially the first layer domains were grown at a constant deposition rate (<0.05 ML/min), keeping the SiO_2 substrate at a constant, elevated temperature of about 80 °C, resulting in very low nucleation density in the first layer. The deposition was stopped at a particular sub-ML coverage when the island sizes were in the order of second layer inter-island separation, when grown at RT. At this coverage, islands sizes were still relatively small in comparison to their separation, making the overlapping of diffusion fields of the neighbors small enough to allow recognition of the initial kinetic shapes of the islands.[13] Subsequently, Pn was deposited at RT with a higher flux (typically 0.1 ML/min). At these deposition conditions, the ES barrier allows for Pn molecules to reach critical concentration for second layer nucleation at the terrace of first layer islands. A LEEM image recorded after the second deposition stage is shown in **Figure 7**. The second layer islands are elongated along the same directions as the bottom layer domains. The kinetic shape anisotropy in Pn is indicative of identical in-plane lattice orientations for both, first and second layers.[13] Micro-beam LEED patterns recorded from first and second layer islands (not shown), provided further evidence for the same in-plane lattice orientation in both layers.

In their study of Pn grown on SiO_2, Kalihari et al.[41] found using transverse shear microscopy (TSM) that the epitaxial

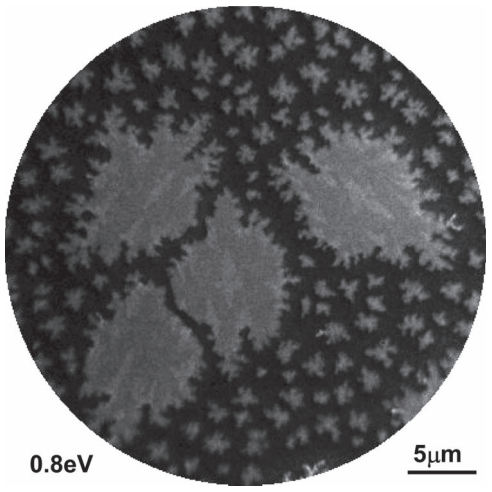

Figure 7. A LEEM image recorded from the second layer islands nucleated in the center of the first layer domain; the second layer islands are elongated along the same directions as the bottom layer domains, indicating identical in-plane lattice orientations for both, first and second layer.

second layer of Pn appeared darker if scanned along [110] crystallographic direction of the first layer, which in turn shows "bright" contrast in the TSM image. This would suggest that in case of the epitaxial growth, the [-110] crystallographic direction in the second layer would have to correspond to [110] direction in the first layer. Our LEEM and μ-LEED results discussed above do not support this hypothesis. Instead we postulate that the inversion of the c*-axis (or "mirror" twinning), which is essentially a molecular tilt switching along alternate diagonals of the Pn in-plane unit cell between the first and second layer islands, is responsible for the contrast formation in the TSM measurements.

To verify the validity of this postulate, we employed LEEM in a dark-field imaging mode to analyze the structure of the Pn islands. In previous work we have shown that an asymmetry in a LEED image, which manifests itself by varying intensity of the equivalent diffraction spots, is associated with molecular tilt and can be employed to differentiate between twinned domains in Pn monolayer on Bi(0001).[19] However, in case of Pn layer on SiO_2 the asymmetry in the LEED pattern is not as prominent, which is due to a very weak diffraction intensity for the spots other than (00), with large background noise resulting from charging effect at the SiO_2 interface, and partly also because of smaller molecular tilt in this system. Nevertheless, by proper choice of the beam tilt and electron energy, certain spots could be made comparable in brightness to the (00) spot. Such tilted dark-field (TDF) LEEM images, taken from the islands shown in bright-field LEEM image in **Figure 8**a are shown in Figures 8b,c. In the bright-field LEEM image shown in Figure 8a, two first layer domains nucleated at close proximity (domain boundary is outlined by a line), having very close in-plane lattice alignments. The dark-field LEEM images in Figure 8b,c show that the second layer islands are twinned in terms of molecular tilt in regard to the first layer, and to each other.

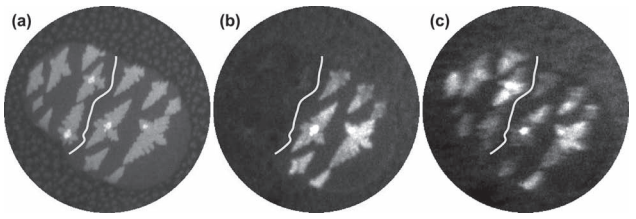

Figure 8. a) Bright-field LEEM image showing second layer islands (bright) on top of two neighboring first layer islands (gray); note that the second layer islands have same in-plane lattice orientations, as it is apparent from their shapes; b,c) tilted bright-field LEEM images for the same area using respectively (11) and (1-1) LEED spots to form the image; The field-of-view is 10 μm for all images, while the imaging electron energy is 1.2 eV, 5 eV and 5.8 eV for (a), (b) and (c), respectively; line depicts the boundary between two different first layer domains that nucleated in a close proximity to each other.

3. Conclusions

It is well established that the interplay between molecule-molecule interaction versus molecule-substrate interaction in organic film growth is a key factor in self assembly processes in nucleation and thin film growth. In the present work we explored the unique capability of LEEM for the real-time investigation of the film growth processes, focusing on the role of molecular reorientation processes in self-assembly of anisotropic molecules, such as pentacene.

We have observed layer-by-layer growth of Pn on SiO_2 substrate, which is different than the expected Volmer–Weber growth mode typical for the systems with lower adhesion (weak interfacial interaction). The observed growth mechanism is also different than conventional concept of layer-by-layer, or Frank van der Merwe growth. In the Pn/SiO_2 system the nucleation density decreases in each consecutive layer, at least up to four monolayers. We call this growth mechanism the inverse Stranski–Krastanov growth. Lower nucleation density in the second layer is associated with inter-layer cohesion being larger than the interfacial adhesion. Such balance makes the molecules less likely to transition to standing-up state from the lying-down configuration while the molecule diffuses on the surface. The gradual lowering of the nucleation density in the subsequent layers continues until the ES barrier starts do dominate the growth processes, and indeed, the Stranski–Krastanov growth mode is observed for the thick Pn films. On the other hand, while Pn is deposited on a substrate with which it interacts more strongly (better adhesion), such as on semiconducting $\alpha\sqrt{3}$-Bi-Si(111), it has a very low nucleation density in the first layer, and the nucleation density in the second layer is several orders of magnitude higher. The observed growth modes could be explained by existence of an energy barrier for Pn nucleation in standing-up orientation, as the molecule needs to reorient itself from a lying-down, diffusing state in order to build into the crystalline film.

In the Pn on SiO_2 growth system, the second layer islands nucleate preferentially at the domain boundaries formed by the interconnections of the bottom (first layer) islands. The top layer overgrows the bottom layer domains with its own initial in-plane crystal orientation, regardless of the in-plane

orientations underlying Pn domains. If the top layer nucleates on the terrace rather than at the domain boundary, it is found to maintain epitaxial relation with the domain on top of which it nucleated.

The bright-field LEEM characteristics and dark-field LEEM imaging allowed us to distinguish between Pn domains having different variation of azimuthal direction of molecular tilt. These observations revealed frequent twinning between first and second Pn layer and between various domains in the second layer islands (inversion of out-plane axis or molecular tilt).

LEEM intensity versus start voltage (LEEM *I–V*) curves taken in the vicinity of mirror potential from the first and second layer Pn islands show that the potential of the second layer is higher by about 0.05 eV in relation to that of the first layer, while there is no difference in the surface potentials for the epitaxial and non-epitaxial parts of the second layer island.

4. Experimental Section

In this study we employed low-energy electron microscopy (LEEM),[39] which has excellent capability of combining the real-time, real-space observations of the film morphology with the crystallographic analysis by means of micro-beam low-energy electron diffraction (μ-LEED). Moreover, use of the low-energy electrons minimizes irradiation damage to the specimen, making this technique especially valuable for studying thin organic films, which are usually prone to irradiation.

Pn was thermally evaporated from a tantalum crucible on native SiO_2/Si(111), in situ in the LEEM system under ultrahigh vacuum, with base pressure in the range of $\approx 5 \times 10^{-10}$ Torr, at deposition rates ranging from 0.01 to 0.1 ML/min. Here, 1 ML (monolayer) corresponds to molecular density in the Pn(001) plane.[5] Prior to Pn deposition, SiO_2 substrates were treated by air plasma. In some experiments we deposited Pn on α 3-Bi-Si(111) and Bi(0001)/Si(111) substrates in the LEEM chamber, in order to evaluate the role of substrate, and thus strength of the substrate-molecule interaction on the growth mechanism of the Pn film. Ultraflat α 3-Bi/Si(111)[13] and Bi(0001)/Si(111) surfaces[42] were grown in situ on a clean Si(111)-7 × 7 surfaces prepared by flash heating at about 1200 °C.

To complement the experimental results, we also computed in-plane molecular packing energies and Pn-Pn interface energies using density functional theory (DFT) calculations. The calculations were done using the DFT Electronic Structure Program, Materials Studio DMol^3,[43,44] version 5.0. Energy of the structure and optimized geometry were obtained in DFT calculation using both, Perdew-Wang (PW) generalized gradient approximation (GGA) functional and PW local density functional (LDA).[45] The orbital cutoffs were set to 3.7 and 3.1 Å for C and H atoms, respectively ("global fine" option in DMol^3). We used periodic structure with two molecules per unit cell (four molecules per unit cell in bilayer calculations). The double numerical plus polarization (DNP) basis set was used and DFT semi-core pseudopotential, an all-electron scalar relativistic pseudopotential (VPSR)[46] was employed for relativistic corrections.

Acknowledgements

The authors would like to thank Dr. Peter Sutter for stimulating discussions. Research carried out at the Center for Functional Nanomaterials and National Synchrotron Light Source, Brookhaven National Laboratory, which are supported by the U.S. Department of Energy, Office of Basic Energy Sciences, under Contract No. DE-AC02-98CH10886.

Received: November 21, 2012
Revised: January 30, 2013
Published online: April 9, 2013

[1] C. D. Dimitrakopoulos, P. R. L. Malenfant, *Adv. Mater.* **2002**, *14*, 99.
[2] A. Virkar, S. Mannsfeld, J. H. Oh, M. F. Toney, Y. H. Tan, G. Liu, J. C. Scott, R. Miller, Z. Bao, *Adv. Funct. Mater.* **2009**, *19*, 1962.
[3] O. D. Jurchescu, J. Baas, T. T. M. Palstra, *Appl. Phys. Lett.* **2004**, *84*, 3061.
[4] a) C. D. Dimitrakopoulos, S. Purushothaman, J. Kymissis, A. Callegari, J. M. Shaw, *Science* **1999**, *283*, 822; b) J. Jang, S. H. Han, *Curr. Appl. Phys.* **2006**, *6*, e17.
[5] a) R. B. Campbell, J. M. Robertson, J. Trotter, *Acta Crystallogr.* **1961**, *14*, 705; b) R. B. Campbell, J. M. Robertson, *Acta Crystallogr.* **1962**, *15*, 289.
[6] C. C. Mattheus, G. A. de Wijs, R. A. de Groot, T. T. M. Palstra, *J. Am. Chem. Soc.* **2003**, *125*, 6323.
[7] J. E. Northrup, M. L. Tiago, S. G. Louie, *Phys. Rev. B* **2002**, *66*, 121404.
[8] J. H. Kang, X.-Y. Zhu, *Appl. Phys. Lett.* **2003**, *82*, 3248.
[9] S. Lukas, S. Söhnchen, G. Witte, C. Wöll, *Chem. Phys. Chem.* **2004**, *5*, 266.
[10] Söhnchen, S. Lukas, G. Witte, *J. Chem. Phys.* **2004**, *121*, 525.
[11] M. Satta, S. Iacobucci, R. Larciprete, *Phys. Rev. B* **2007**, *75*, 155401.
[12] R. Ruiz, B. Nickel, N. Koch, L. C. Feldman, R. F. Haglund, A. Kahn, G. Scoles, *Phys. Rev. B* **2003**, *67*, 125406.
[13] A. Al-Mahboob, J. T. Sadowski, Y. Fujikawa, K. Nakajima, T. Sakurai, *Phys. Rev. B* **2008**, *77*, 035426.
[14] S. Nishikata, G. Sazaki, J. T. Sadowski, A. Al-Mahboob, T. Nishihara, Y. Fujikawa, S. Suto, T. Sakurai, K. Nakajima, *Phys. Rev. B* **2007**, *76*, 165424.
[15] J. T. Sadowski, T. Nagao, S. Yaginuma, Y. Fujikawa, A. Al-Mahboob, K. Nakajima, T. Sakurai, G. E. Thayer, R. M. Tromp, *Appl. Phys. Lett.* **2005**, *86*, 073109.
[16] A. Al-Mahboob, J. T. Sadowski, T. Nishihara, Y. Fujikawa, Q. K. Xue, K. Nakajima, T. Sakurai, *Surf. Sci.* **2007**, *601*, 1304.
[17] Y. Tsuruma, A. Al-Mahboob, S. Ikeda, J. T. Sadowski, G. Yoshikawa, Y. Fujikawa, T. Sakurai, K. Saiki, *Adv. Mater.* **2009**, *21*, 4996.
[18] R. Ruiz, A. Papadimitratos, A. C. Mayer, G. G. Malliaras, *Adv. Mater.* **2005**, *17*, 1795.
[19] A. Al-Mahboob, Y. Fujikawa, J. T. Sadowski, T. Hashizume, T. Sakurai, *Phys. Rev. B* **2010**, *82*, 235421.
[20] A. Al-Mahboob, J. T. Sadowski, T. Nishihara, Y. Fujikawa, Q. K. Xue, K. Nakajima, T. Sakurai, *Surf. Sci.* **2007**, *601*, 1311.
[21] J. T. Sadowski, G. Sazaki, S. Nishikata, A. Al. Mahboob, Y. Fujikawa, K. Nakajima, R. M. Tromp, T. Sakurai, *Phys. Rev. Lett.* **2007**, *98*, 046104.
[22] A. Al-Mahboob, J. T. Sadowski, T. Nishihara, Y. Fujikawa, T. Sakurai, in *Frontiers in Materials Research* (Eds: Y. Fujikawa, K. Nakajima, T. Sakurai), Springer, Berlin/Heidelberg, Germany **2008**, pp. 281–293.
[23] J. T. Sadowski, A. Al-Mahboob, Y. Fujikawa, T. Sakurai, in *Frontiers in Materials Research* (Eds: Y. Fujikawa, K. Nakajima, T. Sakurai), Springer, Berlin/Heidelberg **2008**, pp. 257–279.
[24] G. E. Thayer, J. T. Sadowski, F. Meyer zu Heringdorf, T. Sakurai, R. M. Tromp, *Phys. Rev. Lett.* **2005**, *95*, 256106.
[25] F. C. Frank, J. H. van der Merwe, *Proc. R. Soc. London* **1949**, *A 198*, 205.
[26] I. N. Stranski, L. Von Krastanow, *Akad. Wiss. Lit. Mainz, Math.-Naturwiss. Kl.* **1939**, *146*, 797.
[27] M. Volmer, A. Weber, *Z. Phys. Chem.* **1926**, *119*, 277.
[28] G. Ehrlich, F. G. Hudda, *J. Chem. Phys.* **1966**, *44*, 039.
[29] R. L. Schwoebel, *J. Appl. Phys.* **1969**, *40*, 614.
[30] G. Yoshikawa, J. T. Sadowski, A. Al-Mahboob, Y. Fujikawa, T. Sakurai, Y. Tsuruma, S. Ikeda, K. Saiki, *Appl. Phys. Lett.* **2007**, *90*, 251906.
[31] A. Al-Mahboob, J. T. Sadowski, unpublished.
[32] A. Al-Mahboob, J. T. Sadowski, Y. Fujikawa, T. Sakurai, *Surf. Sci.* **2009**, *603*, L53.
[33] B. Stadlober, U. Haas, H. Maresch, A. Haase, *Phys. Rev. B* **2006**, *74*, 165302.
[34] S. Y. Yang, K. Shin, C. E. Park, *Adv. Funct. Mater.* **2002**, *15*, 1806.

[35] S. E. Fritz, S. M. Martin, C. D. Frisbie, M. D. Ward, M. F. Toney, *J. Am. Chem. Soc.* **2004**, *126*, 4084.
[36] D. Holmes, S. Kumaraswamy, A. Matzeger, K. P. C. Vollhardt, *Chem. Eur. J.* **1999**, *5*, 3399.
[37] H.-L. Cheng, Y.-S. Mai, W.-Y. Chou, L.-R. Chang, X.-W. Liang, *Adv. Funct. Mater.* **2007**, *17*, 3639.
[38] A. C. Mayer, R. Ruiz, H. Zhou, R. L. Headrick, A. Kazimirov, G. G. Malliaras, *Phys. Rev. B* **2006**, *73*, 205307.
[39] E. Bauer, *Rep. Prog. Phys.* **1994**, *57*, 895.
[40] B. Ünal, Y. Sato, K. F. McCarty, N. C. Bartelt, T. Duden, C. J. Jenks, A. K. Schmid, P. A. Thiel, *J. Vac. Sci. Technol. A* **2009**, *27*, 1249.
[41] V. Kalihari, D. J. Ellison, G. Haugstad, C. D. Frisbie, *Adv. Mater.* **2009**, *21*, 3092.
[42] T. Nagao, J. T. Sadowski, M. Saito, S. Yaginuma, Y. Fujikawa, T. Kogure, T. Ohno, Y. Hasegawa, S. Hasegawa, T. Sakurai, *Phys. Rev. Lett.* **2004**, *93*, 105501.
[43] B. Delley, *J. Chem. Phys.* **1990**, *92*, 508.
[44] B. Delley, *J. Chem. Phys.* **2000**, *113*, 7756.
[45] a) J. P. Perdew, Y. Wang, *Phys. Rev. B* **1992**, *45*, 13244; b) J. P. Perdew, Y. Wang, *Phys. Rev. B* **1986**, *33*, 8800; c) J. P. Perdew, *Physica B* **1991**, *172*, 1.
[46] B. Delley, *Phys. Rev. B* **2002**, *66*, 155125.